Regulating Neuroinflammatory Biomarkers in Nitroglycerine induced Migraine in Rats: A Therapeutic role of Chrysanthemum indicum extract

Rapuru Rushendran
SRM Institute of Science and Technology (Deemed to be University) College of Pharmacy
Chitra Vellapandian
SRM Institute of Science and Technology (Deemed to be University) College of Pharmacy
Ilango Kaliappan (ilangok1@srmist.edu.in)
SRM Institute of Science and Technology (Deemed to be University) College of Pharmacy https://orcid.org/0000-0002-0425-9613

Research Article

Keywords: Chrysanthemum indicum, CGRP, Chronic migraine, Herbal treatment, iNOS. Network Pharmacology, Nitroglycerine, Preclinical

Posted Date: June 29th, 2023

DOI: https://doi.org/10.21203/rs.3.rs-3074728/v1

Abstract

Objective

Chronic migraine (CM) is characterised by unilateral/bilateral pulsatile headaches at least 15 days per month. Central sensitization can be demonstrated by a prolonged increase in trigeminal nucleus caudalis (TNC) neuron activity in response to painful stimuli. Scientists are continually researching migraine treatments, hoping herbal remedies may work better. Network pharmacological approach was used to assess *Chrysanthemum indicum* (CIHE) leaf hydroalcoholic extract to evaluate antimigraine activity.

Methods

We investigated specific genes involved in the migraine, extracted gene ontology, biological pathways, and protein-protein interaction analysis were determined with the screened 61 common genes by network pharmacological approach added with docking analysis. *In vivo* studies have been carried out with CD1 Mice (25-30g) randomly made into five groups. CIHE is prepared to evaluate antimigraine activity. MMP9, TNF-α, NFkB, IL-1β, CGRP, and iNOS were evaluated after administration of Nitroglycerine (10mg/kg; i.p).

Results

The elevated protein levels were significantly reduced with the treatment of CIHE (200mg/kg and 400mg/kg; p.o). Additionally histological and western blot analysis confirmed the reduction of specified proteins in the brain as well as blood. Docking analysis revealed that 1,5-Bis(4-dimethylaminophenyl)-1,4-pentadien-3-one (-10.3 KJ/mol), Naphthalene-1-carboxylic acid 4-formyl-phenyl ester (-9.7KJ/mol), and 3-(3-Nitrophenyl)-2'-acrylonaphthone (-9.7KJ/mol) are shown highest binding affinity.

Interpretation:

CIHE may attain antimigraine activity through suppression of neuroinflammatory cytokines by the natural extract of *Chrysanthemum indicum* in a dose dependent manner and isolation of hit molecules from the CIHE is required for further investigation.

Introduction

Network pharmacology is an emerging science based on the network of disease-gene-drug targets, which can provide a deep insight or scientific proof for the drug discovery and allow elucidating the pharmacological mechanism of active components at the molecular level. It is rapidly becoming a holistic and efficient tool for describing the complex interactions between medications and biological systems such as human organs, diseases, metabolic pathways and target proteins [1]. The network pharmacology paradigm, which combines computational prediction and experimental validation, offers a fresh approach to investigating the mechanism of action of individual compounds [2]. Synergistic multi-compound network pharmacology and drug repurposing provide precise and effective therapeutic intervention, eliminating the requirement for drug discovery and speeding up clinical translation [3]. It is one of the new investigational approaches which assists in finding the pathways related to chronic migraine.

Chronic migraine (CM) is a prevalent disabling neurological illness that is defined by unilateral or bilateral pulsatile headache on at least 15 days per month[4]. The WHO has classified it as one of the four most dangerous chronic dysfunctional diseases, causing serious harm to patients' physical and mental health. Central sensitization is now widely considered as one of the key pathogenic processes of CM, manifesting as a persistent increase in the excitability of neurons in the trigeminal nucleus caudalis (TNC) generated by pain stimuli. MMP9, TNF-α, NFkB, IL-1β, CGRP, and iNOS are the specific biomarkers involved in the migraine attack which was diagrammatically represented in Fig. 1. All the marketed drugs such as anti CGRP antagonist, NSAIDs and other pain relieving drugs are available to prevent migraine attack but its having severe cardiac adverse effects which does not allow it to take by most of the persons and very small in quantity will consume on their own risk but a few people stick to roll-on, gels, pain relieving spray, etc. on temporary based [5–7]. So it is suggested that herbal treatment may give a better solution that many herbal plants are not yet scientifically proved for migraine, one among them is *Chrysanthemum indicum* L. (CI) generally known as “Queen of Eastern Ghats”. CI is a perennial plant in the Asteraceae family, has been used as a traditional medicine in China for over 2000 years and is frequently used for the treatment of Pemphigus, swelling, discomfort, and scrofula. More than 190 chemical elements of this plant have been isolated and identified to date, including flavonoids, terpenoids, phenylpropanoids, and phenolic acids [8]. Especially CI is used to relieve headache with decoction of leaves in tribal areas but scientifically not yet proved. Based on this we have further investigated antimigraine activity with CI leaves hydroalcoholic extract by specifically targeting biomarkers such as Calcitonin gene related peptide[9], Nitric oxide Synthase[10], Nuclear factor kappa Beta[11], Interleukin-1 beta[12], Tumour necrotic factor alpha[13], NOD like receptor-3-NLRP3[12, 14, 15], and MMP-9[16]. The rationale of this research, we screened and forecast probable target molecules with their signal pathways for *Chrysanthemum indicum* active components in migraine treatment through network pharmacology and molecular docking. We hope that the natural treatment may give better solution to treat the migraineurs without any adverse effects.

Materials and Methods

Preparation of plant extract and GC-MS finger print analysis

Chrysanthemum indicum plants were collected at local market, Guduvancheri, Tamil Nadu and it was authenticated by Dr. P. Jayaraman, Director, Plant Anatomy Research Center, Tambaram, Chennai, Tamil Nadu (Reg. No. PARC/20224707) (Fig. 2). The leaves were separated, shaded dried, and precautions were taken to avoid contamination during leaf drying. Home mixer was used for making coarse powder (1kg) of raw material and defatted twice with hexane. Then the crude extract (200g) were obtained by extracting with hydroalcoholic extract (Ethanol and water; 70:30) using soxhlet setup, stored in desiccator, and used whenever it required. Based on their molecular weight and retention time, biomolecules present in crude extract were identified using GCMS solution-RT analysis software. The analysis were performed in programmed mode with the following parameters: start temperature 50°C, kept for 5 minutes; programming rate °C/min. = 2, 4, 8, and final temperature 300°C, held for 30 minutes. The sample size was 1µl, and the split ratio was 1:80. Helium was used as the transport gas. The temperature of the injector remained constant at 300°C.

Target Prediction

The chemical components in *Chrysanthemum indicum* (CI) were screened using the ADME parameters such as Molecular weight (MW) ≤ 500, chemical composition with no more than ten hydrogen bond acceptors (HBA ≤ 10), no more than five hydrogen bond donors (HBD ≤ 5), and an octanol-water partition coefficient not more than five (LogP ≤ 5) TPSA 60–140, and Rotatable bonds ≤ 10 were used as the criteria for Lipinski's Rule (LR) of five to identify the active biomolecules. Compounds that did not meet at least two of the aforementioned criteria were not allowed [17, 18]. The flow diagram of the research work has been illustrated in the Fig. 3.

Network Pharmacology of Chrysanthemum indicum

All the chemical structures were prepared and converted into canonical SMILES using PubChem (https://pubchem.ncbi.nlm.nih.gov) and the compound SMILES was then entered into the Swiss Target Prediction (https://www.swisstargetprediction.ch/) to determine the corresponding targets of the main compounds of *Chrysanthemum indicum* and the projected targets for the individual biomolecule were identified by utilizing UniProt ID (https://www.uniprot.org/). Additionally, GeneCard (https://www.genecards.org/) and DisGeNet (https://www.disgenet.org/) were utilized to pull the data related to genes responsible for the migraine.

Gene ontology (GO) and Protein-protein interaction (PPI)

Functional annotations of gene products, including proteins and RNAs, can advance research in many areas, including disease analysis, medication development, gene set enrichment analysis, and many more. High-throughput tests may now be carried out with decreasing costs, and they produce a variety of functional data regarding gene products. Molecular functional ontology (MFO), biological process ontology (BPO), and cellular component ontology (CCO) make up the three ontologies that make up GO. A gene product's fundamental molecular functions, such as binding and catalysis, are described by MFO; the beginning and end of integrated living units, such as cells, tissues, organs, and organisms, are captured by BPO; and the components of cells and their extracellular environments are described by CCO[19, 20]. Using the STRING database to examine protein-protein interactions was our intention. Protein-protein functional and molecular interactions were estimated using STRING online, and Cytoscape analysis was used to search for and choose the master genes[21, 22].

Molecular docking

AutoDock tool 1.5.6 software was used for molecular modelling. The structures of CI compounds were obtained directly from the PubChem database and the crystal structures of the targets such as CGRP (6PFO, 2WCB, and 2WC8) and iNOS (1M8D and 1M9T) were downloaded from the RCSB protein data bank (https://www.rcsb.org/). The selected PDB were screened based on their algorithm (1.5-2.0^{0}A) and A-chain breaking PDB was avoided. The co-crystallized ligand and water molecules were removed from the structure during the protein-making process. H atoms were added, and the side chains were locked in place. Grid generation occurred following the addition of polar hydrogen, the merging of non-polar hydrogens, and the addition of Kollman charges. The receptor was then adjusted to rigid with no flexible connections in order to conduct docking investigations. Docking score represents the binding affinity of ligand and receptor. Biovia Discovery Studio software was utilized for the illustrations of ligand-receptor binding[23, 24].

Experimental Validation

Animals

CD1-Mice (25-30g) were randomly divided in five groups of six in cages with a 12:12hr light/dark cycle at a temperature of 21 ± 1°C and 50 ± 5% humidity. Tap water and the typical laboratory diet were freely available. All experiments on animals were approved by the Institute Animal Ethics Committee (IAEC/268/2021) at SRM College of Pharmacy, SRMIST, and followed the CPCSEA guidelines for the care and use of laboratory animals. We did our best to limit the number of animals used in the experiment and make sure they didn't have to go through too much pain. Before the experiment, all of the animals were given a week to get used to their new environments. Mice were divided equally in five groups and for outcome assessment was done based on a random number sequence made in the Excel software. The animals were weighed every day during the treatment, and no adverse effects were seen.

Nitroglycerine induction and drug administration

Chronic Migraine (CM) was established by the induction of NTG. The diluted NTG (1mg/ml) was freshly prepared with 0.9% saline daily from the stock solution of 5mg/ml. The diluted NTG was introduced to mice (10mg/kg, b.wt) for 9 days (total 5 times) alternatively through intraperitoneally. Mice were divided randomly into five groups: (1) Normal (2) NTG (3) Standard-NTG + Sumatriptan (600µ/kg, b.wt), (4) NTG + Test I (200mg/Kg, b.wt), and (5) NTG + Test II (400mg/kg, b.wt). Mice were sacrificed after 24hrs of last dosing and the rostral spinal cord was taken out and dissected to evaluate satisfied the criteria for histological analysis and Western blot investigation.

Enzyme-linked Immunosorbent assay (ELISA)

CGRP, Nitric oxide, NFkB, ILβ1, and MMP9 levels in the TNC were evaluated using appropriate ELISA kits. PBS (pH 7.2–7.4, 0.01mol/L) was added in a 1:9 proportion to the tissue and homogenised at -30^{0}C. The slurry was then centrifuged at 5000 rpm for 15 minutes to collect the supernatant. Samples were added to the respective microenzyme plate wells and bound with particular antibodies, as directed. The plate was then sealed with a membrane and incubated for 60 minutes at 37^{0}C with HRP-conjugated reagent. After washing the wells with washing buffer, chromogen solutions A and B were applied to each well. Chromogen solutions A and B were exposed to light for 15 minutes at 37^{0}C. Finally check the optical density (OD) at 450nm [7].

Western blot analysis

The tissue was homogenized with buffer and centrifuged at 500xg for 10 minutes at 40^{0}C. The cell pellet was re-suspended in ice-cold PBS and 400µl of ice-cold lysis buffer A to which a cocktail of 4µl protease inhibitor was added. After incubation and centrifugation, remove the fat top layer carefully and collect the remaining supernatant fraction. 400µl of ice-cold lysis buffer B containing 4µl protease inhibitor was added and centrifuged at 7000g. Protein concentration was measured by bicinchoninate assay. 20µg of Protein extract was separated by sodium dodecyl sulphate-polyacrylamide gel electrophoresis and the resolved proteins were transferred to nitrocellulose membranes. Each membrane was incubated with primary anti-CGRP antibody cell signaling (D5R8F) Rabbit # mAb 14959), and Anti-iNOS (D6B6S) Rabbit mAb #13120. Loading Control Anti-Beta Tubulin antibody (Abcam #ab21058) (dilution 1:1000) with Secondary goat anti-rabbit IgG (Thermofisher #31460) (dilution 1:5000)[25, 14].

Statistical analysis

All data are shown as means ± standard deviations (SD). GraphPad Prism version 9.5.0 was used for all statistical analyses and graphs. The mechanical threshold data was statistically analysed using one-way repeated measures analysis of variance (ANOVA), with drug and time as factors. One-way ANOVA was used to analyse the Western blot data, followed by Tukey's multiple comparison test. P value of < 0.05 was considered as significant in all statistical comparisons.

Histopathology

Mice were decapitated, isolate the brain immediately washed in Physiological Salt Solution (PSS) and stored in Formalin solution for further analysis. Brain atlases is used for the location of Hypothalamus region, cut the thin tissue layer, Eosin and Haematoxylin were used as staining agent for imaging the CGRP biomarkers. The pathological changes were observed in all the groups.

Results

Active biomolecules identified in Chrysanthemum indicum

The CIHE was subjected to GC-MS reported 100 biomolecules were found by manually comparing known spectral components to the spectra in a library. Compounds detected in chromatograms of the examined oil are listed (see Table 1) and spectrum was represented in Fig. 4. In order to obtain the primary chemicals in Swiss ADME tool by following Lipinski rule of five. Therefore 20 biomolecules altogether were qualified as the candidate compounds for more thorough research.

Table 1
List of biomolecules GC-MS analysis.

S. no	*Biomolecule*
1	Ethanone, 1 [1,1'-biphenyl] 4-yl
2	Hept-1-en-3-one, 1-(2-naphthyl)
3	Acenaphthene, 5 acetyl
4	Ethanone, 1 [1,1'-biphenyl] 4-yl
5	Ethanone, 1 [1,1'-biphenyl] 4-yl
6	9,12 Octadecadienoic acid, ethyl ester
7	Linoleic acid ethyl ester
8	trans,trans-9,12 Octadecadienoic acid, propyl ester
9	Linoleic acid ethyl ester
10	9,12-Octadecadienoic acid (Z,Z), methyl ester
11	9,12,15-Octadecatrienoic acid, ethyl ester, (Z,Z,Z)
12	Dichloroacetic acid, tridec-2-ynyl ester
13	9,12,15-Octadecatrienoic acid, ethyl ester, (Z,Z,Z)
14	9,12,15-Octadecatrienoic acid, ethyl ester, (Z,Z,Z)
15	Linolenic acid, 2-hydroxy-1 (hydroxymethyl) ethyl ester (Z,Z,Z)
16	3-n-Propyl-2-thiabicyclo [4.4.0]decane (cis,cis)
17	2,5-Dihydro-2-ethyl-2,4-dimethyl-5-oxofuran-3-carboxylic acid
18	2H-1-Benzothiopyran, octahydro-3-propyl (3.alpha., 4a.alpha., 8a.alpha.)
19	3-(3-Nitrophenyl) 2'-acrylonaphthone
20	1,3,3-Trimethyl-2-thiabicyclo [2.2.2]octane
21	2-Naphthamide, N-benzyl-N-pentyl
22	2-Naphthamide, N-benzyl-N (3-methylbutyl)
23	4-Benzyl-2-t-butyl-3 (naphthalene-2-carbonyl) oxazolidin-5-one
24	2,5-Pyrrolidinedione, 1 [(1-naphthalenenylcarbonyl)oxy]
25	3-Phenyl-4-(napht-2-yl-carbonylamino)-4,5 (1H)-dihydro 1,2,4-triazole-5-one
26	N-(2-Methoxy-5-methyl-phenyl)-3 [(naphthalene-1-carbonyl)-hydrazono] butyramide
27	2,2,4-Trimethyl-5-oxo-2,5-dihydro 3 furancarboxylic acid
28	Propenoic acid, 2-cyano-3-[2-(4-nitrophenyl)-1-oxoethylhydrazino], ethyl ester
29	Naphthalene-1-carboxylic acid 4-formyl-phenyl ester
30	1,2-Cyclohexanedicarboxylic acid, 2-isopropylphenyl propyl ester
31	2-Naphthamide, N-benzyl-N-pentyl
32	2-Naphthamide, N-benzyl-N-(3-methylbutyl)
33	4-Benzyl-2-t-butyl-3 (naphthalene-2-carbonyl) oxazolidin-5-one
34	2,5-Pyrrolidinedione, 1-[(1 naphthalenenylcarbonyl)oxy]
35	2,5-Pyrrolidinedione, 1-[(2 naphthalenylcarbonyl)oxy]
36	trans,trans-1,5-Bis (p (dimethylamino) phenyl) 1,4-pentadien-3-one
37	1,5-Bis (4-dimethylamino phenyl) 1,4-pentadien-3-one
38	10-Thia-9-aza tetra cyclo [10.2.1.0(2,11).0(3,8)]pentadeca-3(8),4,6-triene, 5-methyl-, 10,10-dioxide
39	[3.4-c]-phenyl-8-methyl-10,10-dimethyl-5,10,11,11a-tetra hydro-3H-benzo[e]pyrrolo[1,2-a]azepin-3-one
40	Bicyclo [4.1.0]heptan-endo-2-ol, 1-(4-methoxy phenyl)
41	trans,trans-1,5-Bis (p (dimethyl amino) phenyl) 1,4-pentadien-3-one

S. no	*Biomolecule*
42	1,5-Bis (4-dimethyl amino phenyl) 1,4-pentadien-3-one
43	trans-Cinnamamide, 3-trifluoro methyl-N-benzyl-N-methyl
44	4-Cyano-6-(4-fluoro phenyl)pyrimidine
45	4-Acetyl-3-amino-5-propyl-2-cyclo pentene-1,1,2-tricarbonitrile
46	trans,trans-1,5-Bis (p (dimethyl amino)phenyl) 1,4-pentadien-3-one
47	1,5-Bis (4 dimethyl amino phenyl) 1,4-pentadien-3-one
48	trans-Cinnamamide, 3-trifluoro methyl-N-benzyl-N-methyl
49	4-Cyano-6-(4-fluoro phenyl)pyrimidine
50	Pyrimidine, 2-cyano-4-(4-fluoro phenyl)
51	trans,trans-1,5-Bis(p-(dimethyl amino)phenyl)-1,4-pentadien-3-one
52	1,3-Diazaadamantan-6-one, 2-(2-hydroxy phenyl)-5,7-dimethyl
53	Thiophene-3-carboxylic acid, 4,5-dihydro-5 (2-furfurylideno) 4-oxo-2-phenylamino-, ethyl ester
54	1,5-Bis (4-dimethylaminophenyl) 1,4-pentadien-3-one
55	2 (2,4-Dihydroxy phenyl) 5,7-dimethyl-1,3-diazatri cyclo[3.3.1.1(3,7)] decan-6-one
56	4-(3-Amino butyl)-2-methoxyphenol
57	1-Diphenyl(methyl) silyloxy cyclohexane
58	4-(methylthio)benzyl methyl ketoxime
59	1-Piperidineacetonitrile, alpha-phenyl
60	4-Propargylpiperazine-1-carbothioic acid 2-[1-[2-pyridyl]ethylidene]
61	trans,trans-1,5-Bis (p (dimethyl amino)phenyl) 1,4-pentadien-3-one
62	1,5-Bis (4 dimethyl amino phenyl) 1,4-pentadien-3-one
63	3-Ethyl-2 (3-nitrostyryl) 4-quinazolone
64	1,2-Propanediol, 3-bromo-2-phenyl
65	2-butanone, 1,4-dibromo-3-hydroxy-3-phenyl
66	trans,trans-1,5-Bis (p (dimethyl amino)phenyl) 1,4-pentadien-3-one
67	1,5-Bis (4 dimethyl amino phenyl) 1,4-pentadien-3-one
68	Benzaldehyde, 3-bromo-4-hydroxy
69	Benzene, 4-bromo-1-methoxy-2-neryl
70	Iron, [(1,2,3,4,5-.eta.) 2,4-cyclohexadien-1-yl](.eta.5 – 2,4-cyclo pentadien-1-yl)
71	trans,trans-1,5-Bis (p (dimethyl amino)phenyl) 1,4-pentadien-3-one
72	1,5-Bis (4 dimethyl amino phenyl) 1,4-pentadien-3-one
73	Propenoic acid, 2-cyano-3-[3,6-dihydro-2,2-dimethyl-4-morpholino-2H-pyran-5-yl], ethyl ester
74	Bicyclo [4.1.0]heptan-endo-2-ol, 1-(4-methoxyphenyl)
75	Pregna-1,4,16-triene-3,20-dione, 11,22-diacetoxy
76	trans,trans-1,5-Bis (p (dimethyl amino)phenyl) 1,4-pentadien-3-one
77	1,5-Bis (4 dimethyl amino phenyl) 1,4-pentadien-3-one
78	Estra-1,3,5(10)-trien-17-one, 16,16-difluoro-3-methoxy
79	Estra-1,3,5(10)-trien-17-one, 16,16-difluoro-3-methoxy
80	Estra-1,3,5(10)-trien-17-one, 16,16-difluoro-3-methoxy
81	trans,trans-1,5-Bis (p (dimethyl amino)phenyl) 1,4-pentadien-3-one
82	1,5-Bis (4 dimethyl amino phenyl) 1,4-pentadien-3-one
83	Estra-1,3,5(10)-trien-17-one, 16,16-difluoro-3-methoxy
84	trans-Cinnamamide, 3-trifluoromethyl-N-benzyl-N-methyl

S. no	*Biomolecule*
85	Estra-1,3,5(10)-trien-17-one, 16,16-difluoro-3-methoxy
86	trans,trans-1,5-Bis (p (dimethyl amino)phenyl) 1,4-pentadien-3-one
87	1,5-Bis (4 dimethyl amino phenyl) 1,4-pentadien-3-one
88	Estra-1,3,5(10)-trien-17-one, 16,16-difluoro-3-methoxy
89	trans-Cinnamamide, 3-trifluoromethyl-N-benzyl-N-methyl
90	4-Cyano-6-(4-fluorophenyl)pyrimidine
91	1,5-Bis(4-dimethylaminophenyl)-1,4-pentadien-3-one
92	trans,trans-1,5-Bis(p-(dimethyl amino)phenyl)-1,4-pentadien-3-one
93	Estra-1,3,5(10)-trien-17-one, 16,16-difluoro-3-methoxy
94	trans-Cinnamamide, 3-trifluoro methyl-N-benzyl-N-methyl
95	Estra-1,3,5(10)-trien-17-one, 16,16-difluoro-3-methoxy
96	trans,trans-1,5-Bis (p (dimethyl amino)phenyl) 1,4-pentadien-3-one
97	1,5-Bis (4 dimethyl amino phenyl) 1,4-pentadien-3-one
98	Estra-1,3,5(10)-trien-17-one, 16,16-difluoro-3-methoxy
99	Estra-1,3,5(10)-trien-17-one, 16,16-difluoro-3-methoxy
100	trans-Cinnamamide, 3-trifluoromethyl-N-benzyl-N-methyl

Anti-migraine target screening using Chrysanthemum indicum components

The targets for the 20 biomolecules with 417 targets were obtained from Swiss Target Prediction. Targets from each component were compared and mapped to their human homologs to eliminate any redundancies and collected all the information from DisGeNet, and GeneCard databases (443 targets). The results of the gene mapping sets revealed 61 common targets from migraine coincided with CIHE, DisGeNet, and GeneCard databases.

Protein-protein interaction network analysis

Highly interconnected nodes in a network are typically shared biological components or pathways. The link between the two nodes (genes/proteins) was provided for 61 major hub nodes that were chosen and added into the STRING database. Figure 5 shows the PPI network (61 nodes and 302 edges). TYMS does not interact with other targets. A score of 0.70 or higher indicates high confidence. Two distinct nodes with high combined value of more than 0.90 were listed in (Supplementary I**)** such as APP and BAEC1, TRPV1 and TRPA1, TRPV1 and TRPM8, TRPV1 and CNR1, TRPV3 and TRPM8, APP and RELA, TRPV1 and FAAH etc.

Gene ontology analysis

The gene ontology enrichment analysis, which included three parts such as biological process (BP), cellular components (CC), and molecular functioning (MF), was used to further investigate the significance of 61 common genes by using String database. GO enrichment analysis of the 61 putative targets of enriched terms in biological process (631), cellular component (51), and molecular function (65) categories. The level of statistical significance was set at $p < 0.05$. The top ten significantly enriched terms in the biological process, molecular function, and cellular components were illustrated in Fig. 6 and degree analysis was listed out in Table 2.

Table 2
Degree analysis of Compound-Target-Pathway.

Gene	*Degree*	*Closeness Centrality*	*Betweenness Centrality*
PIK3CA	22	0.41	0.07
PTGS2	15	0.40	0.05
P2RX7	12	0.41	0.03
HTR2A	11	0.40	0.02
MAOB	10	0.39	0.01
Biomolecule	**Degree**	**Closeness Centrality**	**Betweenness Centrality**
Mol 37	22	0.38	0.06
Mol 28	19	0.40	0.06
Mol 19	16	0.39	0.04
Mol 2	14	0.36	0.03
Mol 9	14	0.41	0.05
Mol 44	14	0.37	0.03
Mol 12	13	0.35	0.01
Kegg ID	**Degree**	**Closeness Centrality**	**Betweenness Centrality**
hsa04080	23	0.46	0.10
hsa04020	12	0.42	0.03
hsa04726	11	0.42	0.03
hsa04024	9	0.36	0.00
hsa04728	9	0.36	0.01
hsa04750	7	0.36	0.00
hsa04926	7	0.39	0.01
hsa04015	7	0.39	0.01

KEGG pathway enrichment analysis

The 61 potential active chemical targets were mapped onto the 89 KEGG pathways (p-value < 0.05) and detailed information is available in Supplementary-II. The top 20 paths (p-value < 0.005) were chosen and arranged by p-value from largest to smallest, as shown (see Table 3). Neuroactive ligand-receptor interaction, cAMP Signaling pathway, serotonergic synapse, dopaminergic synapse, NFkB and ILβ-1 pathway etc., are may be the targeted pathways for migraine attack and major proteins such as CACNA1C, iNOS2, CGRP, TRPV1, NLRP3, MMP9 are involved in it. The KEGG enrichment pathway analysis was represented in Fig. 7. Multiple compounds from CI act on the same target protein, and a single compound acts on multiple target proteins and multiple pathways. This shows the synergistic effect of "multiple components, multiple targets, and multiple pathways" of CI.

Table 3
Biological pathways of migraine.

Kegg ID	*Pathways*	*Observed gene count*	*Background gene count*	*Strength*	*Matching proteins*
hsa05030	Cocaine addiction	7	49	1.66	SLC6A3, DRD2,MAOA,MAOB,GRIN2A,RELA,GRIN2B
hsa04726	Serotonergic synapse	13	108	1.59	SLC6A4,CACNA1C,HTR2C,APP,HTR5A,HTR1A,HTR7,MAOA,PTGS2,HTR1B,HTR1D,M
hsa00360	Phenylalanine metabolism	2	17	1.58	MAOA, MAOB
hsa00350	Tyrosine metabolism	4	35	1.56	MAOA, COMT, MAOB, DBH
hsa00340	Histidine metabolism	2	21	1.48	MAOA, MAOB
hsa05031	Amphetamine addiction	6	66	1.46	CACNA1C,SLC6A3,MAOA,MAOB,GRIN2A,GRIN2B
hsa04728	Dopaminergic synapse	11	128	1.44	DRD4,CACNA1C,SLC6A3,DRD5,MAOA,COMT,DRD2,MAOB,DRD3,GRIN2A,GRIN2B
hsa04080	Neuroactive ligand-receptor interaction	25	330	1.39	DRD4,HTR2C,HTR5A,DRD5,F2,EDNRA,HTR1A,P2RX7,HTR7,HRH3,DRD2, CNR1,HTR1B,HTR1D,EDNRB,DRD3,GRIN2A,HCRTR1,OPRM1,AGTR1,HTR2A,TRPV1 GRIN2B,HCRTR2,ADRA2B
hsa04750	Inflammatory mediator regulation of TRP channels	7	94	1.38	TRPA1,PIK3CA,HTR2C,TRPV3,TRPM8,HTR2A,TRPV1
hsa04930	Type II diabetes mellitus	3	46	1.32	PIK3CA,CACNA1C,INSR
hsa01523	Antifolate resistance	2	31	1.32	TYMS,RELA
hsa04020	Calcium signaling pathway	12	193	1.3	CACNA1C,HTR2C,HTR5A,DRD5,EDNRA,NOS2,P2RX7,HTR7,EDNRB,GRIN2A,AGTR1
hsa04742	Taste transduction	5	81	1.3	CACNA1C,HTR1A,HTR1B,HTR1D,SCN2A
hsa00330	Proline and Arginine metabolism	3	48	1.3	NOS2,MAOB,MAOA
hsa04933	AGE-RAGE signaling pathway in diabetic complications	6	98	1.29	MMP2,PIK3CA,ICAM1,TGFBR2,RELA,AGTR1
hsa04913	Ovarian steroidogenesis	3	50	1.28	INSR,PTGS2,CYP19A1
hsa04917	Prolactin signaling pathway	4	69	1.27	PIK3CA,ESR2,RELA,ESR1
hsa05140	Leishmaniasis	4	70	1.26	NOS2,PTGS2,TLR4,RELA
hsa04923	Regulation of lipolysis in adipocytes	3	54	1.25	PIK3CA,INSR,PTGS2
hsa04926	Relaxin signaling pathway	7	128	1.24	MMP2,PIK3CA,NOS2,TGFBR2,MMP9,EDNRB,RELA
hsa04668	TNF signaling pathway	6	112	1.24	PIK3CA,ICAM1,MMP3,PTGS2,MMP9,RELA
hsa04960	Aldosterone-regulated sodium reabsorption	2	37	1.24	PIK3CA,INSR
hsa04024	cAMP signaling pathway	11	208	1.23	PIK3CA,CACNA1C,DRD5,EDNRA,HTR1A,DRD2,HTR1B,HTR1D,GRIN2A,RELA,GRIN2I

Kegg ID	*Pathways*	*Observed gene count*	*Background gene count*	*Strength*	*Matching proteins*
hsa04915	Estrogen signaling pathway	7	133	1.23	MMP2,PIK3CA,PGR,ESR2,MMP9,OPRM1,ESR1
hsa01522	Endocrine resistance	5	95	1.23	MMP2,PIK3CA,ESR2,MMP9,ESR1
hsa00260	Serine, Glycine and threonine metabolism	2	38	1.23	MAOB,MAOA
hsa05033	Nicotine addiction	2	38	1.23	GRIN2A,GRIN2B
hsa05215	Prostate cancer	5	96	1.22	PIK3CA,MMP3,MMP9,RELA,FGFR2
hsa05142	Chagas disease	5	99	1.21	PIK3CA,NOS2,TGFBR2,TLR4,RELA
hsa00380	Tryptophan metabolism	2	41	1.19	MAOA,MAOB
hsa05219	Bladder cancer	2	41	1.19	MMP2,MMP9
hsa04066	HIF-1 signaling pathway	5	106	1.18	PIK3CA,INSR,NOS2,TLR4,RELA
hsa04929	GnRH secretion	3	63	1.18	PIK3CA,CACNA1C,ESR2
hsa04720	Long-term potentiation	3	64	1.18	CACNA1C,GRIN2A,GRIN2B
hsa04927	Cortisol synthesis and secretion	3	65	1.17	CACNA1C,KCNK2,AGTR1
hsa04924	Renin secretion	3	66	1.16	CACNA1C,EDNRA,AGTR1
hsa04657	IL-17 signaling pathway	4	92	1.14	MMP3,PTGS2,MMP9,RELA
hsa05222	Small cell lung cancer	4	92	1.14	PIK3CA,NOS2,PTGS2,RELA
hsa05144	Malaria	2	46	1.14	ICAM1,TLR4
hsa05034	Alcoholism	6	144	1.13	SLC6A3,MAOA,DRD2,MAOB,GRIN2A,GRIN2B
hsa05212	Pancreatic cancer	3	73	1.12	PIK3CA,TGFBR2,RELA
hsa05146	Amoebiasis	4	100	1.11	PIK3CA,NOS2,TLR4,RELA
hsa05133	Pertussis	3	74	1.11	NOS2,TLR4,RELA
hsa05220	Chronic myeloid leukemia	3	75	1.11	PIK3CA,TGFBR2,RELA
hsa04064	NF-kappa B signaling pathway	4	101	1.1	ICAM1,PTGS2,TLR4,RELA
hsa05418	Fluid shear stress and atherosclerosis	5	130	1.09	MMP2,PIK3CA,ICAM1,MMP9,RELA
hsa04961	Endocrine and other factor-regulated calcium reabsorption	2	53	1.08	ESR1,VDR
hsa04022	cGMP-PKG signaling pathway	6	162	1.07	CACNA1C,INSR,EDNRA,EDNRB,AGTR1,ADRA2B
hsa04670	Leukocyte transendothelial migration	4	109	1.07	MMP2,PIK3CA,ICAM1,MMP9
hsa04015	Rap1 signaling pathway	7	202	1.05	PIK3CA,INSR,DRD2,CNR1,GRIN2A,FGFR2,GRIN2B
hsa05323	Rheumatoid arthritis	3	85	1.05	ICAM1,MMP3,TLR4

Kegg ID	*Pathways*	*Observed gene count*	*Background gene count*	*Strength*	*Matching proteins*
hsa04211	Longevity regulating pathway	3	87	1.04	PIK3CA,INSR,RELA
hsa04540	Gap junction	3	87	1.04	HTR2C,DRD2,HTR2A
hsa05235	PD-L1 expression and PD-1 checkpoint pathway in cancer	3	88	1.04	PIK3CA,TLR4,RELA
hsa04713	Circadian entrainment	3	92	1.02	CACNA1C,GRIN2A,GRIN2B
hsa04014	Ras signaling pathway	7	226	1	PIK3CA,INSR,HTR7,GRIN2A,RELA,FGFR2,GRIN2B
hsa05161	Hepatitis B	5	159	1	PIK3CA,TGFBR2,MMP9,TLR4,RELA
hsa04620	Toll-like receptor signaling pathway	3	101	0.98	PIK3CA,TLR4,RELA
hsa04625	C-type lectin receptor signaling pathway	3	102	0.97	PIK3CA,PTGS2,RELA
hsa05010	Alzheimer disease	10	355	0.96	PIK3CA,CACNA1C,APP,INSR,BACE1,NOS2,PTGS2,GRIN2A,RELA,GRIN2B
hsa05145	Toxoplasmosis	3	105	0.96	NOS2,TLR4,RELA
hsa04723	Retrograde endocannabinoid signaling	4	145	0.95	FAAH,CACNA1C,PTGS2,CNR1
hsa05224	Breast cancer	4	145	0.95	PIK3CA,PGR,ESR2,ESR1
hsa04931	Insulin resistance	3	107	0.95	PIK3CA,INSR,RELA
hsa05200	Pathways in cancer	14	517	0.94	MMP2,PIK3CA,F2,EDNRA,NOS2,ESR2,TGFBR2,PTGS2,MMP9,EDNRB,RELA,ESR1,F
hsa04072	Phospholipase D signaling pathway	4	147	0.94	PIK3CA,INSR,F2,AGTR1
hsa04724	Glutamatergic synapse	3	111	0.94	CACNA1C,GRIN2A,GRIN2B
hsa05167	Kaposi sarcoma associated herpesvirus infection	5	187	0.93	PIK3CA,ICAM1,CCR1,PTGS2,RELA
hsa05205	Proteoglycans in cancer	5	196	0.91	MMP2,PIK3CA,MMP9,TLR4,ESR1
hsa04380	Osteoclast differentiation	3	122	0.9	PIK3CA,TGFBR2,RELA
hsa05164	Influenza A	4	165	0.89	PIK3CA,ICAM1,TLR4,RELA
hsa05135	Yersinia infection	3	125	0.89	PIK3CA,TLR4,RELA
hsa05152	Tuberculosis	4	168	0.88	NOS2,TLR4,RELA,VDR
hsa05202	Transcriptional misregulation in cancer	4	171	0.88	MMP3,TGFBR2,MMP9,RELA
hsa04068	FoxO signaling pathway	3	127	0.88	PIK3CA,INSR,TGFBR2
hsa04270	Vascular smooth muscle contraction	3	133	0.86	CACNA1C,EDNRA,AGTR1
hsa05017	Spinocerebellar ataxia	3	135	0.85	PIK3CA,GRIN2A,GRIN2B

Kegg ID	*Pathways*	*Observed gene count*	*Background gene count*	*Strength*	*Matching proteins*
hsa04062	Chemokine signaling pathway	4	186	0.84	PIK3CA,CCR2,CCR1,RELA
hsa05162	Measles	3	138	0.84	PIK3CA,TLR4,RELA
hsa05226	Gastric cancer	3	144	0.82	PIK3CA,TGFBR2,FGFR2
hsa04932	Non alcoholic fatty liver disease	3	148	0.81	PIK3CA,INSR,RELA
hsa04218	Cellular senescence	3	150	0.81	PIK3CA,TGFBR2,RELA
hsa04934	Cushing syndrome	3	153	0.8	CACNA1C,KCNK2,AGTR1
hsa05166	Human T-cell leukemia virus 1 infection	4	211	0.78	PIK3CA,ICAM1,TGFBR2,RELA
hsa05163	Human cytomegalovirus infection	4	218	0.77	PIK3CA,CCR1,PTGS2,RELA
hsa04010	MAPK signaling pathway	5	288	0.75	CACNA1C,INSR,TGFBR2,RELA,FGFR2
hsa05012	Parkinson disease	4	240	0.73	SLC6A3,MAOA,DRD2,MAOB
hsa05020	Prion disease	4	265	0.68	PIK3CA,CACNA1C,GRIN2A,GRIN2B
hsa04151	PI3K-Akt signaling pathway	5	350	0.66	PIK3CA,INSR,TLR4,RELA,FGFR2

Docking analysis

Before the experimental analysis, a ligand binding simulation was executed to see if the 20 CI biomolecules could directly bind to the selected proteins CGRP and iNOS are majorly involved in migraine attack compare to other biomarkers. 1,5-Bis(4-dimethylaminophenyl)-1,4-pentadien-3-one (-10.3KJ/mol), Naphthalene-1-carboxylic acid 4-formyl-phenyl ester (-9.7KJ/mol) and 3-(3-Nitrophenyl)-2'-acrylonaphthone (-9.7KJ/mol) are shown highest binding affinity among others shown (Table 4 and Fig. 8). These data suggested that more than half of the CI biomolecules may have a substantial potential to directly connect with iNOS and CGRP, because molecular docking is still a computer simulation approach used to predict the shape of a receptor-ligand complex and the hypothesis needs be tested empirically in future investigations. The molecule 13 formed a hydrogen bond with amino acid residues THR 127, THR 75 and TRP 118 in CGRP. The Molecule 19 formed a hydrogen bond with amino acid residues CYS 194, ARG 193, PRO 192, ALA 191, TRP 188, MET 349, LEU 203 and PHE 363 in target of iNOS. The Molecule 30 formed a hydrogen bond with amino acid residues ASP 77, CYS 72, GLY 116, VAL 117, TRP 118, TRP 128, SER 129 and TYR 131 in CGRP. Each target ligand created at least one hydrogen bond with active chemical residues, lending credence to the accuracy and precision of the prediction made by the research.

Table 4
Binding affinity of CGRP and iNOS proteins of 20 compounds.

Biomolecule	*Structure*	*CGRP*		*iNOS*		
		6PFO	*2WCB*	*2WC8*	*1M8D*	*1M9T*
Ethanone, 1-[1,1'-biphenyl]-4-yl		-8.22	-5.97	-4.73	-7.12	-5.6
Hept-1-en-3-one, 1-(2-naphthyl)-		-8.7	-6.75	-4.92	-8.73	-6.89
Acenaphthene, 5-acetyl		-7.55	-6.43	-4.65	-7.71	-7.65
Linolenic acid, 2-hydroxy-1-(hydroxymethyl)ethyl ester (Z,Z,Z)-		-7.44	-4.45	-1.67	-4.93	-5.52
2H-1-Benzothiopyran, octahydro-3-propyl- (3.alpha., 4a.alpha., 8a.alpha.)-		-7.66	-6.23	-4.66	-7.13	-7.22
3-(3-Nitrophenyl)-2'-acrylonaphthone		-10.1	-7.9	-6.78	-9.7	-9.39
Naphthalene-1-carboxylic acid 4-formyl-phenyl ester		-9.3	-7.35	-4.67	-9.7	-9.57
1,2-Cyclohexanedicarboxylic acid, 2-isopropylphenyl propyl ester		-8.65	-7.1	-3.87	-8.72	-8.57
2,5-Pyrrolidinedione, 1-[(1-naphthalenenylcarbonyl)oxy]-		-8.7	-7.46	-4.78	-8.78	-8.7
2,5-Pyrrolidinedione, 1-[(2-naphthalenylcarbonyl)oxy]-		-8.45	-7.43	-4.59	-8.8	-8.74
10-Thia-9-azatetracyclo[10.2.1.0(2,11).0(3,8)]pentadeca-3(8),4,6-triene, 5-methyl-, 10,10-dioxide		-8.3	-7.11	-5.42	-7.82	-7.67
[3.4-c]-phenyl-8-methyl-10,10-dimethyl-5,10,11,11a-tetrahydro-3H-benzo[e]pyrrolo[1,2-a]azepin-3-one		-9.84	-8	-5.46	-9.03	-8.83
Bicyclo[4.1.0]heptan-endo-2-ol, 1-(4-methoxyphenyl)-		-7.32	-6.08	-4.49	-6.87	-6.5
1,5-Bis(4-dimethylaminophenyl)-1,4-pentadien-3-one		-10.36	-6.52	-4.78	-9.3	-9.03
Pyrimidine, 2-cyano-4-(4-fluorophenyl)-		-7.75	-6.4	-4.7	-6.7	-6.04
1,3-Diazaadamantan-6-one, 2-(2-hydroxyphenyl)-5,7-dimethyl		-7.99	-6.7	-6.05	-8.42	-7.71
4-(3-Aminobutyl)-2-methoxyphenol		-5.82	-6.4	-5.06	-6	-5.26
1-Piperidineacetonitrile, .alpha.-phenyl		-7.2	-6.03	-4.9	-6.98	-6.9
2-butanone, 1,4-dibromo-3-hydroxy-3-phenyl		-6.06	-4.67	-3.48	-6.08	-5.96
Estra-1,3,5(10)-trien-17-one, 16,16-difluoro-3-methoxy		-9.23	-6.23	-5.33	-8.91	-8.73

Effect of CIHE on Nitroglycerin induced mice

Reliability of the mouse model was assessed by measuring the protein levels of matrix metalloproteinase 9 (MMP9), NFkB, IL-1β, and TNF. For 11 days, mice were given daily doses of Sumatriptan (600µg/kg, b.wt i.p) and CIHE (200mg/kg and 400mg/kg, b.wt p.o). NTG was administered to mice on days 1, 3, 5, 7, and 9, and daily sumatriptan and CIHE therapy significantly decreased NTG-induced basal hypersensitivity and acute hyperalgesia. In comparison to the NTG-induced group, Sumatriptan and CIHE dramatically reduced the protein expression levels of TNF, IL-1β, MMP9, and NFkB shown (see Table 5**)** and illustrated in Fig. 9.

Table 5
Estimation of biomarkers in NTG induced animal model.

% Inhibition				
Groups	**TNF-α**	**MMP9**	**NFkB**	**IL1-β**
Normal	10.24 ± 0.40	9.78 ± 0.55	17.95 ± 4.77	11.92 ± 5.73
NTG induced (10mg/kg)	48.38 ± 12.03	25.86 ± 0.13	29.59 ± 0.81	39.47 ± 2.32
Test I (200mg/kg)	23.65 ± 3.48*	21.73 ± 5.15*	20.73 ± 0.21*	27.71 ± 0.71*
Test II (400mg/kg)	19.51 ± 0.14**	12.82 ± 0.95**	19.67 ± 0.53**	21.05 ± 0.41**
Sumatriptan (600µg/kg)	14.06 ± 0.90***	10.86 ± 3.49***	21.22 ± 0.45***	16.14 ± 1.95***

Chronic migraine treatment with Sumatriptan and CIHE attenuated the increased protein expression levels of TNF, MMP9, NFkB, and IL1-β. Statistical analyses were performed by one-way ANOVA, followed by a Multiple t-test; ***p < 0.001, **p < 0.002, *p < 0.33 vs. NTG induced group (n = 6 mice per group).

Histopathology analysis

The CGRP biomarkers are highly presence in the Nitroglycerin induced group but it reduced significantly in treated groups which is illustrated in the Fig. 10. The histological report reveals that the CIHE may have antimigraine activity in a dose dependent manner.

Discussion

Our results suggesting that the CIHE attenuates the biomarkers such as MMP9[16], TNF-α[26], NFkB[27], IL-1β[28], CGRP[29], and iNOS[30] are involved in the migraine attack which represented in (Fig. 1). Migraine is one of the critical neurological disorders highly affecting women and children throughout the globe. Now a days migraine like condition being seen frequently with suffering from severe pain associated with different symptoms include phonophobia, photophobia, nausea, vomit, especially fatigue and blindness in severe cases[31]. In the current scenario, the available marketed drugs are giving relief from pain in temporary based associated with risky cardiac adverse effects that lead to sudden death. After literature survey, to eradicate this issue we decided and step forward through natural therapy for migraine. The migraine trigger by NTG can produce symptoms very similar to those experienced by people with chronic migraine. Bioactivation of NTG yields nitric oxide (NO), which may react with peroxide *in vivo* to produce peroxynitrite (PN), which has been linked to the aetiology of migraines. We employed a mouse model of chronic migraine that has been well acknowledged, and it was created by administering NTG (10mg/kg) repeatedly through intraperitoneally considering as universal accepted animal model for migraine. Recently it also revealed that NLRP3 is playing a crucial role in the activation and maturation of IL-1β and suggesting NLRP3 promising target for the migraine[12, 14, 25].

Researchers have hypothesised that oestrogen plays a role in why migraines are more common in women. Numerous studies have demonstrated that oestrogen fluctuations mediate neuronal activity and alter pain signalling transmitters such Gamma Aminobutyric acid (GABA) and serotonin[32]. In order to provide a reliable model of NTG-induced (10mg/kg b.wt) chronic migraine without the confounding effects of oestrogen, male mice were used. Although traditional tribal peoples have long relied on a decoction of CI leaves to alleviate headache pain but it was not scientifically proved with the leaves. *Chrysanthemum indicum* is selectively taken for this intensive research work and due to the presence of phytochemical constituents such as bioflavonoids, terpenoids, phenylpropanoids, phenolic Acids, etc. [8] may play a critical role in the treatment of migraine.

Our results supplement the chronic migraine research in several ways. In this research, NTG induced an increase in the expression of the proinflammatory cytokines IL-1β, TNF-α, NFkB, MMP9, CGRP, and iNOS. This model's validity was tested by assessing the biomarkers responsible for migraine attack which activates the central sensitization were confirmed by measuring MMP9, TNF-α, NFkB, IL-1β, CGRP, and iNOS.

First we screened 20 biomolecules and pulled all the required data computationally from GC-MS analysis through Swiss ADME and Swiss target prediction by Network Pharmacology. The docking studies were carried out with these selected proteins CGRP (PDB ID: 6PFO, 2WCB, and 2WC8) and iNOS (PDB ID: 1M8D and 1M9T) are involved in the migraine. The highest binding affinity was observed in CGRP-6PFO with the biomolecule 1,5-Bis(4-dimethylaminophenyl)-1,4-pentadien-3-one is -10.3KJ/mol and iNOS-1M8D with the biomolecule 3-(3-Nitrophenyl)-2'-acrylonaphthone is − 9.71KJ/mol. So, by this docking results confirms that CHIE having capacity to bind with the migraine biomarkers such as CGRP and iNOS specifically.

Further screening has been elucidated to find specific target proteins involved in migraine attack using DisGeNet and GeneCard databases associated with GC-MS data, we pulled all the required information regarding the genes involved in the migraine. In total, 61 common genes are screened from the data bases are illustrated in Fig. 11 using Bioinformatics and Evolutionary Genomics tool and followed by Protein-Protein Interaction (PPI) enrichment was evaluated that Cellular Components-51, Biological Processes-631, Molecular Function-65, PPI (61 nodes, 302edges, and $p < 1.0e-16$), and 89 Kegg pathways from the String database.

Furthermore, the antimigraine activity was evaluated by different parameters estimated in the NTG inducing animal model (*in vivo*). Enzyme linked Immunosorbent Assay reported that initially MMP9, TNF-α, NFkB, and IL-1β biomarkers are highly elevated but significantly reduced with the treatment of Sumatriptan (600µg/kg b.wt) and CIHE (200mg/kg and 400mg/kg b.wt). We also analysed the effects of CIHE on CGRP and iNOS protein expression in the brain, those involved in the pain pathways. NTG-injection was associated with a trend toward expressed CGRP and iNOS compared to the control, test, and sumatriptan groups by keeping housing gene as β-tubulin with this protein expression analysis convincingly satisfied that CIHE may act as antimigraine by dwindle the biomarkers responsible for the migraine attack. The histopathological report reveals that CGRP observed more clearly in the disease control group but in the sumatriptan and test groups were significantly diminish after treating with CIHE. It is suggesting that CIHE may have antimigraine activity by inhibiting further CGRP synthesis and other proinflammatory molecules such as MMP9, TNF-α, NFkB, and IL-1β in a dose dependent manner without any side effects.

Compound-Target-Pathway network analysis

According to the results of the KEGG analysis, the primary pathways involved in the use of CI in the treatment of migraines are those involving neuroactive ligand-receptor interactions, calcium signalling pathways, cancer-related pathways, cyclic AMP signalling pathways and PI3K-Akt signalling networks represented in the Fig. 12 by using Cytoscape software 3.9.1. The nervous system relies on a complex network of intracellular and extracellular signalling channels, including receptors and ligands localised on the plasma membrane. Pain signals are sent to the brain via these pathways, which entail the production and release of transmitters at synapses and the interaction of these transmitters with receptors. Gene mutations in the calcium signalling pathway have been found to be significantly connected with the aetiology of migraine. This system is also involved in a wide range of neurodegenerative and neuropsychiatric illnesses. There is a specific level of expression for cAMP (cyclic adenosine monophosphate) response element binding protein (CREB) in all brain cells. Central sensitization, which is associated with depression and pain, is mediated by a large number of CREB target genes. The PI3K/Akt signalling pathway has been discovered to be active in rat models of migraine brain tissue. NF-kB is a key route in the migraine disease process, as it is involved in mediating neurogenic inflammation and upregulating the release of downstream inflammatory mediators.

Conclusion

In discussing emerging findings indicates that the expression of CGRP, iNOS, and proinflammatory biomarkers such as MMP9, TNF- α, NFkB, and IL-1β were elevated in a mice model of migraine associated pain generated by repeated NTG stimulation. By inhibition of these biomarkers may reduce hyperalgesia

associated with central sensitization of CM in the TNC. Collectively, these studies add to our understanding of the physiopathology of CM. The *Chrysanthemum indicum* hydroalcoholic extract may regulate CM associated pain and it inhibits the inflammatory molecules may represent a novel therapeutic rationale and strategy for the treatment of migraine using a natural extract. 1,5-Bis(4-dimethylaminophenyl)-1,4-pentadien-3-one may act as a hit/lead molecule in the treatment of migraine but, it requires further *in vitro* and *in vivo* analysis with the isolated biomolecule especially targeting CGRP, iNOS and NLRP3.

Declarations

Statements and Declarations

Funding

The research work was financially supported by giving the National Fellowship by Ministry of Tribal Affairs, Government of India. Award number: **202122-NFST-AND-00924**.

Competing Interests

The authors have no relevant financial or non-financial interests to disclose

Author Contributions

All authors contributed to the study conception and design. Material preparation, data collection and analysis were performed by Rapuru Rushendran; Interpreted, data analysis, supervised, validation, and data compilation by Kaliappan Ilango and Vellapandian Chitra. The first draft of the manuscript was written by Rapuru Rushendran and all authors commented on previous versions of the manuscript. All authors read and approved the final manuscript

Data availability

All information gathered or deduced from this study, along with any relevant online appendices, can be found in this report. If you have any additional questions, please contact the author who wrote the article and the data are available from the corresponding author on reasonable request

Ethics approval

All animal experiments performed were approved by the Ethics Committee for Animal Experimentation of SRM Institute of Science and Technology and conducted in accordance with the CPSCEA guidelines. The ethical approval reference number is IAEC/268/2021.

Consent to Participate

Not applicable

Consent to Publish

Not applicable

Acknowledgement

All the authors would like to express their gratitude to The Management, SRM College of Pharmacy, SRMIST, Kattankulathur, Chengalpattu, Tamil Nadu, India and especially R. Rushendran expresses gratitude to The Honourable President of India, Smt. Droupadi Murmu and Ministry of Tribal Affairs, Government of India for providing fellowship.

References

1. Zhu W, Li Y, Zhao J, Wang Y, Li Y, Wang Y (2022) The mechanism of triptolide in the treatment of connective tissue disease-related interstitial lung disease based on network pharmacology and molecular docking. Annals Med 54(1):541–552. https://doi.org/10.1080/07853890.2022.2034931
2. Zhou W, Zhang H, Wang X, Kang J, Guo W, Zhou L, Liu H, Wang M, Jia R, Du X, Wang W, Zhang B, Li S (2022) Network pharmacology to unveil the mechanism of Moluodan in the treatment of chronic atrophic gastritis. Phytomed 95:153837. https://doi.org/0.1016/j.phymed.2021.153837
3. Nogales C, Mamdouh ZM, List M, Kiel C, Casas AI, Schmidt H (2022) Network pharmacology: curing causal mechanisms instead of treating symptoms. Trends Pharmacol Sci 43(2):136–150. https://doi.org/10.1016/j.tips.2021.11.004
4. Dodick DW (2018) Migraine. Lancet 391(10127):1315–1330. https://doi.org/10.1016/s0140-6736(18)30478-1
5. Inoue K, Tsuda M (2018) Microglia in neuropathic pain: cellular and molecular mechanisms and therapeutic potential. Nat Rev Neurosci 19(3):138–152. https://doi.org/10.1038/nrn.2018.2
6. Iyengar S, Johnson KW, Ossipov MH, Aurora SK (2019) CGRP and the Trigeminal System in Migraine. Headache 59(5):659–681. https://doi.org/10.1111/head.13529
7. Wen Q, Wang Y, Pan Q, Tian R, Zhang D, Qin G, Zhou J, Chen L (2021) MicroRNA-155-5p promotes neuroinflammation and central sensitization via inhibiting SIRT1 in a nitroglycerin-induced chronic migraine mouse model. J Neuroinflamm 18(1):1–25. https://doi.org/10.1186/s12974-021-02342-5

8. Shao Y, Sun Y, Li D, Chen Y (2020) Chrysanthemum indicum L.: A Comprehensive Review of its Botany, Phytochemistry and Pharmacology. Am J Chin Med 48(4):871–897. https://doi.org/10.1142/s0192415x20500421
9. Edvinsson L (2021) CGRP and migraine: from bench to bedside. Rev Neurol 177(7):785–790. https://doi.org/10.1016/j.neurol.2021.06.003
10. Casili G, Lanza M, Filippone A, Campolo M, Paterniti I, Cuzzocrea S, Esposito E (2020) Dimethyl fumarate alleviates the nitroglycerin (NTG)-induced migraine in mice. J Neuroinflamm 17(1):1–16. https://doi.org/10.1186/s12974-020-01736-1
11. Ala M, Mohammad Jafari R, Ala M, Agbele AT, Hejazi SM, Tavangar SM, Mahdavi SRM, Dehpour AR (2020) Sumatriptan alleviates radiation-induced oral mucositis in rats by inhibition of NF-kB and ERK activation, prevention of TNF-α and ROS release. Archives Oral Biol 119:104919. https://doi.org/10.1016/j.archoralbio.2020.104919
12. He W, Long T, Pan Q, Zhang S, Zhang Y, Zhang D, Qin G, Chen L, Zhou J (2019) Microglial NLRP3 inflammasome activation mediates IL-1β release and contributes to central sensitization in a recurrent nitroglycerin-induced migraine model. J Neuroinflamm 16(1):1–17. https://doi.org/10.1186/s12974-019-1459-7
13. Oliveira AB, Bachi ALL, Ribeiro RT, Mello MT, Tufik S, Peres MFP (2017) Unbalanced plasma TNF-α and IL-12/IL-10 profile in women with migraine is associated with psychological and physiological outcomes. J Neuroimmunol 313:138–144. https://doi.org/10.1016/j.jneuroim.2017.09.008
14. Wang Y, Shan Z, Zhang L, Fan S, Zhou Y, Hu L, Wang Y, Li W, Xiao Z (2022) P2X7R/NLRP3 signaling pathway-mediated pyroptosis and neuroinflammation contributed to cognitive impairment in a mouse model of migraine. J Headache Pain 23(1):1–23. https://doi.org/10.1186/s10194-022-01442-8
15. Yuan H, Lu B, Ji Y, Meng B, Wang R, Sun D, Liu R, Zhai X, Li X, Qin J, Chen J (2022) Role of P2X4/NLRP3 Pathway-Mediated Neuroinflammation in Perioperative Neurocognitive Disorders. Mediators Inflamm 2022:6355805. https://doi.org/10.1155/2022/6355805
16. Karademir F, Ozturk M, Altunkaynak Y, Doventas Y, Mutluay B, Basoglu Koseahmet F, Baybas S (2022) [Assessment of serum MMP-9, TIMP-1 levels and MMP-9/TIMP-1 ratio in migraine patients with and without aura]. Ideggyogyaszati Sz 75(9–10):341–349. https://doi.org/10.18071/isz.75.0341
17. Daina A, Michielin O, Zoete V (2017) SwissADME: a free web tool to evaluate pharmacokinetics, drug-likeness and medicinal chemistry friendliness of small molecules. Sci Rep 7:42717. https://doi.org/10.1038/srep42717
18. Daina A, Michielin O, Zoete V (2014) iLOGP: a simple, robust, and efficient description of n-octanol/water partition coefficient for drug design using the GB/SA approach. J Chem Information Modeling 54(12):3284–3301. https://doi.org/10.1021/ci500467k
19. Zhao Y, Wang J, Chen J, Zhang X, Guo M, Yu G (2020) A Literature Review of Gene Function Prediction by Modeling Gene Ontology. Front Genet 11:1–15. https://doi.org/10.3389/fgene.2020.00400
20. Wei Y, Zhai Y, Liu X, Jin S, Zhang L, Wang C, Zou H, Hu J, Wang L, Jiang J, Shen X, Pang L (2022) Long non-coding RNA MIR31HG as a prognostic predictor for malignant cancers: A meta- and bioinformatics analysis. J Clin Laboratory Analysis 36(1):e24082. https://doi.org/10.1002/jcla.24082
21. Karoii DH, Azizi H, Amirian M (2022) Signaling Pathways and Protein-Protein Interaction of Vimentin in Invasive and Migration Cells: A Review. Cell Reprogramming 24(4):165–174. https://doi.org/10.1089/cell.2022.0025
22. Crosara KTB, Moffa EB, Xiao Y, Siqueira WL (2018) Merging in-silico and in vitro salivary protein complex partners using the STRING database: A tutorial. J Proteom 171:87–94. https://doi.org/10.1016/j.jprot.2017.08.002
23. Siva Kumar B, Anuragh S, Kammala AK, Ilango K (2022) Computer Aided Drug Design Approach to Screen Phytoconstituents of Adhatoda vasica as Potential Inhibitors of SARS-CoV-2 Main Protease Enzyme. Life 12(2):1–24. https://doi.org/10.3390/life12020315
24. Ilango KaPL (2023) Identification of phytoconstituents for combating Polycystic ovarian syndrome through in silico techniques
25. Filippone A, Scuderi SA, Basilotta R, Lanza M, Casili G, Bova V, Paterniti I, Esposito E (2022) BAY-117082-driven NLRP3 inflammasome inhibition resolves nitro-glycerine (NTG) neuronal damage in in vivo model of migraine. Biomed Pharmacotherapy 156:113851. https://doi.org/10.1016/j.biopha.2022.113851
26. Zhu J, Chen J, Zhang K (2022) Clinical effect of flunarizine combined with duloxetine in the treatment of chronic migraine comorbidity of depression and anxiety disorder. Brain Behav 12(8):e2689. https://doi.org/10.1002/brb3.2689
27. Latif K, Khan AU, Izhar Ul Haque M, Naeem K (2021) Bergapten Attenuates Nitroglycerin-Induced Migraine Headaches through Inhibition of Oxidative Stress and Inflammatory Mediators. ACS Chem Neurosci 12(18):3303–3313. https://doi.org/10.1021/acschemneuro.1c00146
28. Honarvar NM, Soveid N, Abdolahi M, Djalali M, Hatami M, Karzar NH (2021) Anti-Neuroinflammatory Properties of n-3 Fatty Acids and Nano- Curcumin on Migraine Patients from Cellular to Clinical Insight: A Randomized, Double-Blind and Placebo-Controlled Trial. Endocr Metab Immune Disorders Drug Targets 21(2):365–373. https://doi.org/10.2174/1871530320666200729144430
29. Vandervorst F, Van Deun L, Van Dycke A, Paemeleire K, Reuter U, Schoenen J, Versijpt J (2021) CGRP monoclonal antibodies in migraine: an efficacy and tolerability comparison with standard prophylactic drugs. J Headache Pain 22(1):1–11. https://doi.org/10.1186/s10194-021-01335-2
30. Yang S, Chen C, Liu X, Kang Q, Ma Q, Li P, Hu Y, Li J, Gao J, Wang T, Wang W (2022) Xiongshao Zhitong Recipe Attenuates Nitroglycerin-Induced Migraine-Like Behaviors via the Inhibition of Inflammation Mediated by Nitric Oxide Synthase. Front Pharmacol 13:920201. https://doi.org/10.3389/fphar.2022.920201
31. Goadsby PJ, Holland PR, Martins-Oliveira M, Hoffmann J, Schankin C, Akerman S (2017) Pathophysiology of Migraine: A Disorder of Sensory Processing. Physiol Rev 97(2):553–622. https://doi.org/10.1152/physrev.00034.2015
32. Paredes S, Cantillo S, Candido KD, Knezevic NN (2019) An Association of Serotonin with Pain Disorders and Its Modulation by Estrogens. Int J Mol Sci 20(22):1–21. https://doi.org/10.3390/ijms20225729

Figures

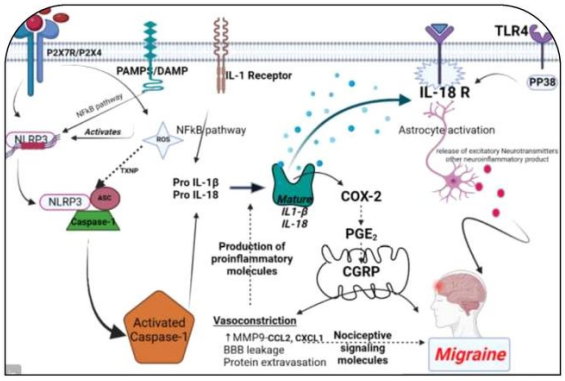

Fig. 1 Relevance of NLRP3 and MMP9 during migraine attack. Production and maturation of proinflammatory signalling molecules through the P2X7R, P2X4, PAMPs or DAMP, TLR4, IL-1β and IL-18 receptor activation. CGRP is released and responsible for vasoconstriction by maturation of IL-1β. In other hand, increase in MMP9, BBB leakage and protein extravasation due to vasoconstriction which is responsible for the further production of proinflammatory molecules. Astrocyte activation plays one of the important roles in release of excitatory neurotransmitters and other neuroinflammatory molecules in the brain which all collectively responsible for migraine attack. The figure was created with BioRender.com.

Figure 1

See image above for figure legend.

Fig. 2 Collection and authentication of *Chrysanthemum indicum* plant

Figure 2

See image above for figure legend.

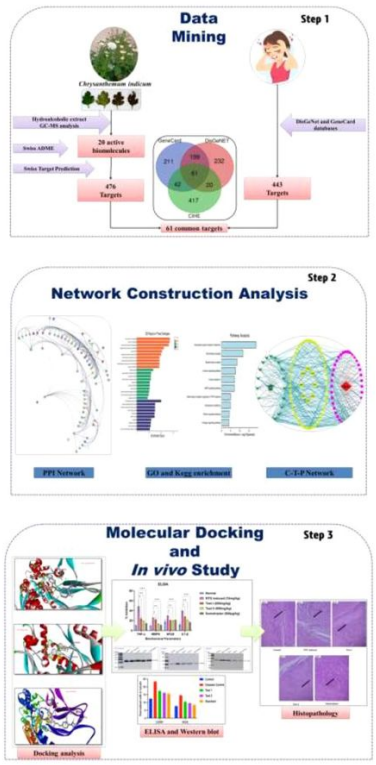

Fig. 3 The flow diagram of research

Figure 3

See image above for figure legend.

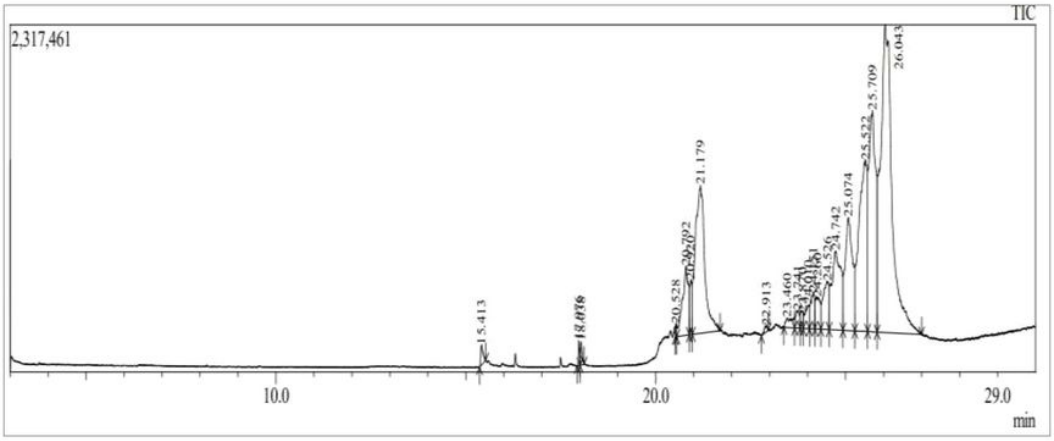

Fig. 4 GC-MS Spectrum analysis

Figure 4

See image above for figure legend.

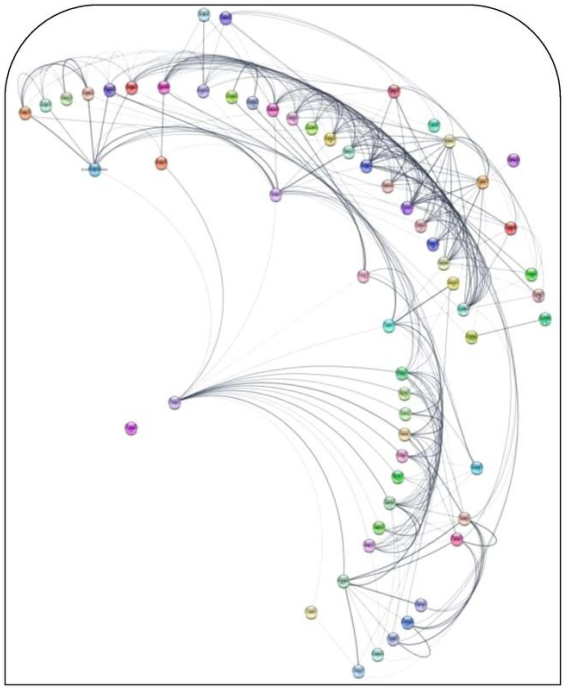

Fig. 5 Migraine targeting PPI network (61 nodes, 302 edges) from STRING. Average node degree: 9.9, Average local clustering coefficient: 0.546, and PPI enrichment p-value: <1.0e-16. PPI network (61 nodes, 302 edges) from Cytoscape 3.9.1. Network nodes and edges represent proteins and protein-protein associations.

Figure 5

See image above for figure legend.

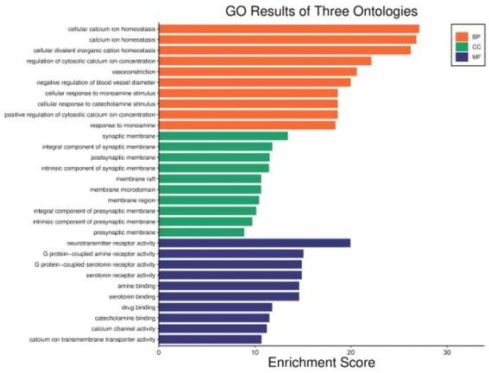

Fig. 6 Gene ontology analysis of screened genes

Figure 6

See image above for figure legend.

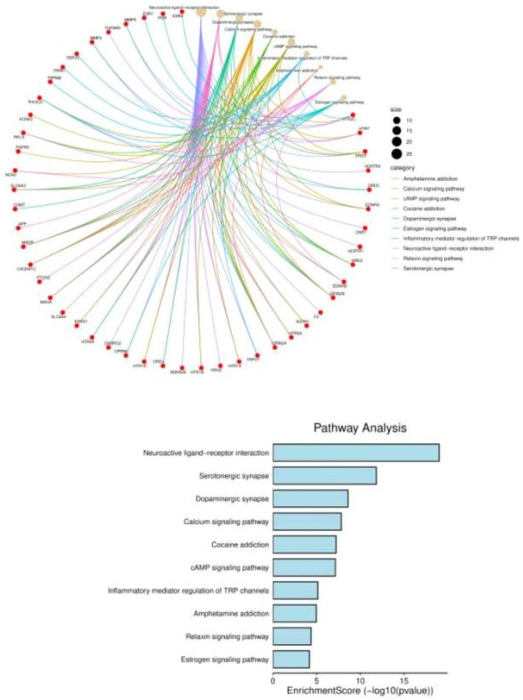

Fig. 7 KEGG pathway enrichment analysis

Figure 7

See image above for figure legend.

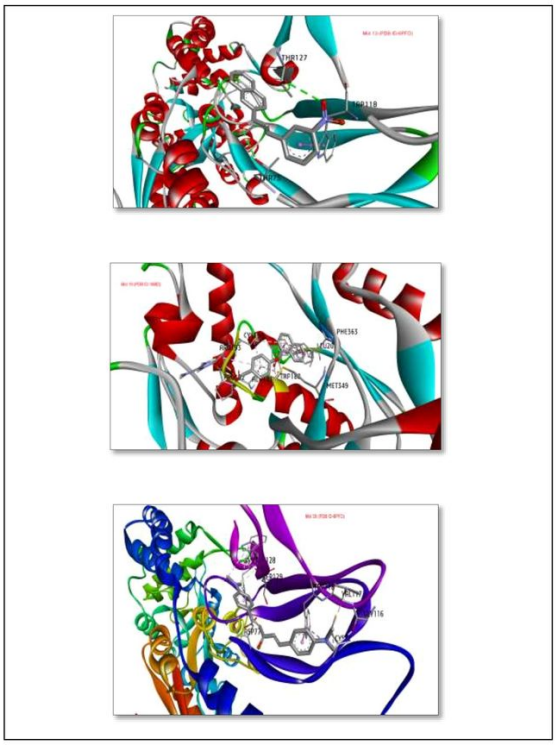

Fig. 8 Docking analysis of Molecule 13, 19 and 30

Figure 8

See image above for figure legend.

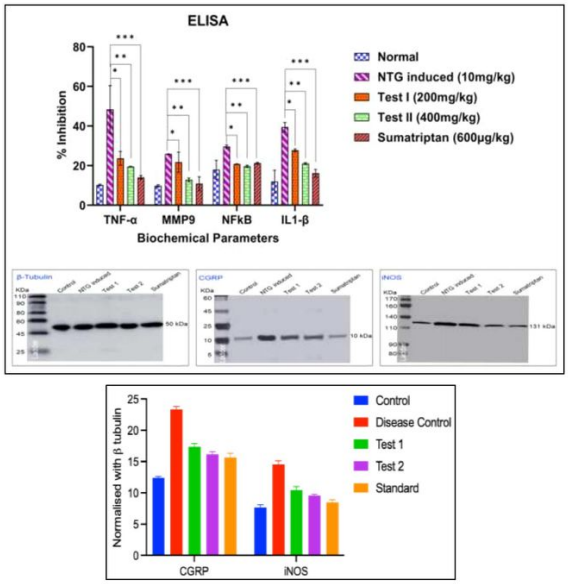

Fig. 9 The percentage inhibition of TNF, MMP9, NFkB, and IL1-β and CGRP and iNOS protein expression. Repeated NTG administration increased the expression of TNF, MMP9, NFkB, and IL1-β. When compare to NTG inducing group all the estimated biomarkers have been reduced after treatment. Chronic treatment with CIHE of CGRP and iNOS proteins expression were tested by western blot on the repeated induction of NTG (n=6 mice per group). The protein expression was significantly attenuated in the treatment groups (Test 1, Test 2, and Sumatriptan) when compare to NTG induced and β-Tubulin is considered as housing gene. Statistical analyses were performed by one-way ANOVA, followed by a Multiple t-test; ***$p < 0.001$, **$p < 0.002$, *$p < 0.33$ vs. NTG induced group (n = 6 mice per group).

Figure 9

See image above for figure legend.

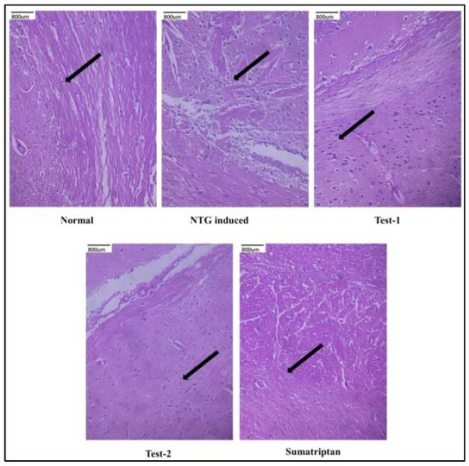

Fig. 10 Brain histological representation of repeated NTG induction model for Chronic Migraine. CGRP observed highly in NTG induced group and significantly reduced in the treatment groups such as Sumatriptan and CIHE groups (Test-1 and Test-2).

Figure 10

See image above for figure legend.

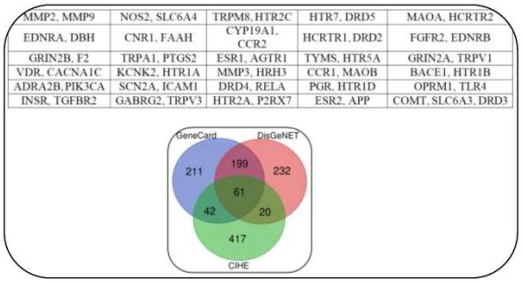

Fig. 11 Common migraine targeting genes. 61 common genes were found with GeneCard, DisGeNET, and CIHE genetical data using Bioinformatics and Evolutionary Genomics tool.

Figure 11

See image above for figure legend.

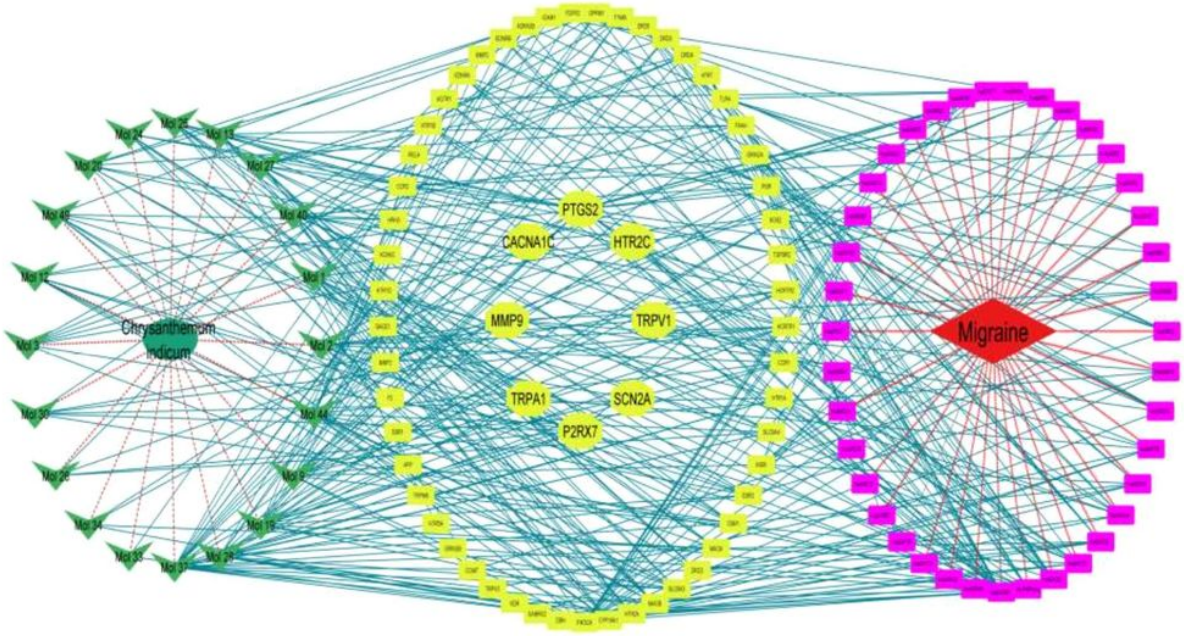

Fig. 12. Compound-target-Pathway networking analysis

Figure 12

See image above for figure legend.

Supplementary Files

This is a list of supplementary files associated with this preprint. Click to download.

- SupplementaryFile1NodeAnnotation.xlsx
- SupplementaryFile2GeneOntology.xlsx